Persistence length of a polyelectrolyte in salty water: a Monte-Carlo study

T. T. Nguyen and B. I. Shklovskii

Theoretical Physics Institute, University of Minnesota,
116 Church Street Southeast, Minneapolis, Minnesota 55455

We address the long standing problem of the dependence of the electrostatic persistence length l_e of a flexible polyelectrolyte (PE) on the screening length r_s of the solution within the linear Debye-Hückel theory. The standard Odijk, Skolnick and Fixman (OSF) theory suggests $l_e \propto r_s^2$, while some variational theories and computer simulations suggest $l_e \propto r_s$. In this paper, we use Monte-Carlo simulations to study the conformation of a simple polyelectrolyte. Using four times longer PEs than in previous simulations and refined methods for the treatment of the simulation data, we show that the results are consistent with the OSF dependence $l_e \propto r_s^2$. The linear charge density of the PE which enters in the coefficient of this dependence is properly renormalized to take into account local fluctuations.

PACS numbers: 61.25.Hq, 87.15.Bb, 36.20.Ey, 87.15.Aa

I. INTRODUCTION

Despite numerous theoretical studies of polyelectrolyte (PE), due to the long range nature of the Coulomb interaction, the description of their conformation is still not as satisfactory as that of neutral polymers. One of the longest standing problem is related to the electrostatic effect on the rigidity of a PE. In a water solution with monovalent ions, within the Debye-Hückel linear screening theory, the electrostatic interaction between PE charged monomers has the form:

$$V(r) = \frac{e^2}{Dr} \exp\left(-\frac{r}{r_s}\right) , \qquad (1)$$

where r is the distance between monomers, D is the dielectric constant of water, e is the elementary charge, and r_s is the Debye-Hückel screening length, which is related to the ionic strength I of the solution by $r_s^2 = 4\pi l_B I$. ($l_B = e^2/Dk_BT$ is the Bjerrum length, T is the temperature of the solution).

The rigidity of a polymer is usually characterized by one parameter, the so called persistence length l_p. For a polyelectrolyte chain, besides the intrinsic persistence length l_0 which results from the specific chemical structure of the monomers and bonds between them, the total persistence length also includes an "electrostatic" contribution l_e which results from the screened Coulomb interactions between monomers:

$$l_p = l_0 + l_e . \qquad (2)$$

Because the interaction (1) is exponentially screened at distances larger than r_s, early works concerning the structure of the PE assumed that l_e is of the order of r_s. However, this simple assumption was challenged by the pioneering works of Odijk[1] and Skolnick and Fixman[2] (OSF), who showed that Debye-Hückel interaction can induce a rod-like conformation at length scales much larger than r_s. Their calculation gives

$$l_e = l_{OSF} = \frac{\eta_0^2}{4Dk_BT} r_s^2 , \qquad (3)$$

where η_0 is the linear charge density of the PE. Because $l_e \propto r_s^2$, it can be much larger than r_s at weak screening (large r_s).

Although the idea that electrostatic interaction enhances the stiffness of a PE is qualitatively accepted and confirmed in many experiments, the quadratic dependence of l_e on the screening length r_s is still the subject of many discussions. In the work of OSF, the bond angle deflection was assumed to be small everywhere along the chain, what is valid for large l_0. They suggested that if l_0 is not small but l_e is large enough (week screening), their assumption is still valid. Ref. 3, however, has questioned this assumption especially when l_0 is so small that the bond angle deflection is large before electrostatics comes into play and rigidifies the chain.

A significant progress was made by Khokhlov and Khachaturian (KK) who proposed a generalized OSF theory[4] for the case of flexible polyelectrolyte (small l_0). It is known that in the absence of screening ($r_s \to \infty$), the structure of a polyelectrolyte can be conveniently described by introducing the concept of electrostatic blobs. A blob is a chain subunit within which the electrostatic interaction is only a weak perturbation. The blob size ξ is related to the number of Kuhn segments g within one blob as $\xi = l_0 g^{1/2}$. The condition of weak Coulomb interaction suggest that the electrostatic self energy of a blob, $(\eta_0 g l_0)^2/D\xi$ is of the order of k_BT. This leads to $\xi \simeq (Dk_BTl_0^2/\eta_0^2)^{1/3}$. At length scale greater than ξ, Coulomb interaction plays important role and the string of blobs assumes a rod-like conformation, with the end-to-end distance proportional to the number of blobs.

Using this blob picture, KK proposed that OSF theory is still applicable for a flexible PE provided one deals with the chain of blobs instead of the original chain of monomers. This means, in Eq. (3), one replaces the bare linear charge density η_0 by that of the blob chain

$\eta = \eta_0 g l_0/\xi$. The intrinsic persistence length l_0 should also be replaced by ξ. As a result, the total persistence length of the flexible PE reads:

$$l_{p,KK} = \xi + \frac{\eta^2}{4Dk_BT} r_s^2 \ . \qquad (4)$$

Thus, in KK theory, despite the flexibility of the PE, its electrostatic persistence length remains quadratic in r_s. Small l_0 only renormalizes the linear charge density from η_0 to η.

Note that r_s is implicitly assumed to be larger than the blob size ξ in KK theory (weak screening). For strong screening $r_s < \xi$, there are no electrostatic rigidity and the chain behaves as flexible chain with the Debye-Hückel short range interaction playing the role of an additional excluded volume interaction.

A number of variational calculations have also been proposed to describe more quantitatively the structure of flexible chain. These calculations, although based on different ansatz, have the same basic idea of describing the flexible charged chain by some model of noninteracting semiflexible chain and variationally optimizing the persistence length of the noninteracting system. Surprisingly, while some of these calculations support the OSF-KK dependence $l_e \propto r_s^2$ such as Refs. 5,6,7, other calculations found that l_e scales linearly with r_s instead[3,8,9]. However, because variational calculation results depend strongly on the variational model Hamiltonian, none of these results can be considered conclusive.

Computer simulations[10,11,12,13,14,15] also have been used to determine the dependence l_e on r_s and to verify OSF or variational theories. Some of these papers claim to support the linear dependence of l_p on r_s. The simulation of Ref. 15 concludes that the dependence of l_p on r_s is sublinear. Thus, the problem of the dependence $l_e(r_s)$, despite being very clearly stated, still remains unsolved for a flexible PE. More details about the present status of this problem can be found in Ref. 16.

In this paper, we again use computer simulations to study the dependence of l_e on r_s. The longest polyelectrolyte simulated in our paper contains 4096 charged monomers, four times more than those studied in previous simulations. This allows for better studying of size effect on the simulation result. Furthermore, we use a more refined analysis of the simulation result, which takes into account local fluctuations in the chain at short distance scale. Our results show that OSF formula quantitatively describes the structure of a polyelectrolyte.

The paper is organized as follows. The procedure of Monte-Carlo simulation of a polyelectrolyte using the primitive freely jointed beads is described in the next section. The data for the end-to-end distance R_{ee} is given. In Sec. III, we analyze this data using the scaling argument to show that it is consistent with OSF theory. In Sec. IV, we analyze the data for the case of large r_s, where excluded volume effect is not important, in order to extract l_e and again show that it obeys OSF theory in this limit. In Sec. V, we use the bond angle correlation function to calculate l_e and to confirm the result of Sec. IV. The good agreement between l_e calculated using different methods further suggests that OSF theory is correct in describing a polyelectrolyte structure. We conclude in Sec. VI.

Several days after the submission of our paper to the Los Alamos preprint archive[17], another paper[18] with Monte-Carlo simulations for PE molecules in the same range of lengths appears in the same archive. Results of this paper are in good agreement with our Sec. III.

II. MONTE-CARLO SIMULATION

The polyelectrolyte is modeled as a chain of N freely jointed hard spherical beads each with charge e. The bond length of the PE is fixed and equal to l_B, where $l_B = e^2/Dk_BT$ is the Bjerrum length which is about 7Å at room temperature in water solution. Thus the bare linear charge density of our polyelectrolyte is $\eta_0 = e/l_B$. Because we are concerned about the electrostatic persistence length only, the bead radius is set to zero so that all excluded volume of monomers is provided by the screened Coulomb interaction between them only. For convenience, the middle bead is fixed in space.

To relax the PE configuration globally, the pivot algorithm[19] is used. In this algorithm, in an attempted move, a part of the chain from a randomly chosen monomer to one end of the chain is rotated by a random angle about a random axis. This algorithm is known to be very efficient. A new independent sample can be produced in a computer time of the order of N, or in other words, uncorrelated samples are obtained every few Monte Carlo (MC) steps (one MC step is defined as the number of elementary moves such that, on average, every particle attempts to move once). To relax the PE configuration locally, the flip algorithm is used. In this algorithm, a randomly chosen monomer is rotated by a random angle about the axis connecting its two neighbor (if it is one of the end monomers, its new position is chosen randomly on the surface of a sphere with radius l_B centered at its neighbor.) In a simulation, the number of pivot moves is about 30% of the total number of moves. The usual Metropolis algorithm is used to accept or reject the move. About $1 \div 2 \times 10^4$ MC steps are run for each set of parameters (N, r_s), of which 512 initial MC steps are discarded and the rest is used for statistical average (due to time constrain, for $N = 4096$, only 2000 MC steps are used). Two different initial configurations, a Gaussian coil and a straight rod, were used to ensure that final states are indistinguishable and the systems reaches equilibrium.

The simulation result for the end-to-end distance R_{ee} of a polyelectrolyte for different N is plotted in Fig. 1 as a function of the screening radius r_s of the solution. At very small r_s, Coulomb interactions between monomers are strongly screened and the chain behaves as a neutral Gaussian chain with $R_{ee} = l_B\sqrt{N-1}$. At very large

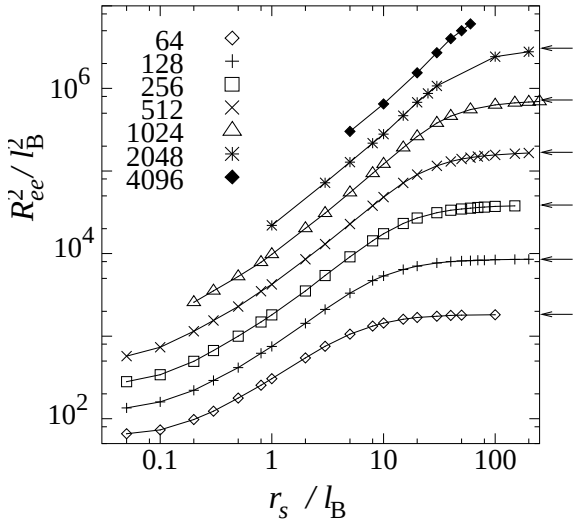

FIG. 1: The square of the end-to-end distance of a polyelectrolyte R_{ee}^2 as a function of the screening length r_s for chains with different number of monomers N: 64($\diamond$), 128(+), 256 ($\Box$), 512 ($\times$), 1024 ($\triangle$), 2048($*$), and 4096 ($\blacklozenge$). The arrows on the right side show R_{ee}^2 obtained using unscreened Coulomb potential $V(r) = e/r$.

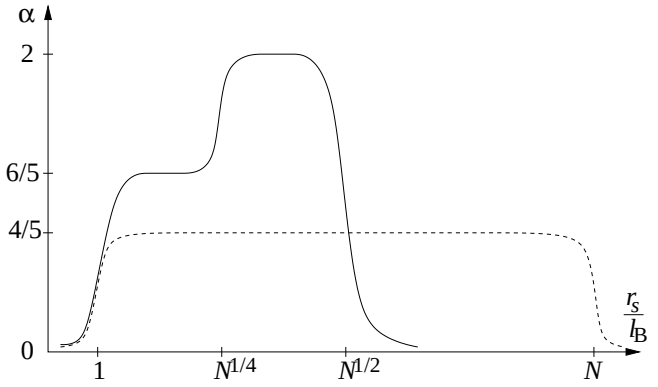

FIG. 2: Schematic plot of α as a function of r_s for the OSF theory $l_p \propto r_s^2$ (solid line) and for variational theories $l_p \propto r_s$ (dashed line).

$r_s \gg N$, Coulomb interactions between the monomers are not screened and R_{ee} is saturated and equal to that of an unscreened PE with the same number of monomers (see the arrows in Fig. 1).

Three different methods are used to verify the validity of OSF theory for flexible PE: i) study of the scaling dependence of R_{ee} on r_s in whole range of r_s, ii) extraction of l_e in the large r_s limit and iii) analysis of the bond correlation function. In the next three sections, we discuss these methods in details together with their limitations. Comparison with previous simulations is also made to explain their results which so far have not supported either of the theories.

III. SCALING DEPENDENCE OF R_{ee} ON r_s

Let us first describe theoretically how the chain size should behave as a function of the screening radius r_s when r_s increases from 0 to ∞.

When $r_s \ll l_B$, the Coulomb interaction is strongly screened. Because there are no other interaction present in our chain model of freely jointed beads, the chain statistic is Gaussian. Its end-to-end distance R_{ee} is proportional to the the square root of the number of bonds and independent on r_s:

$$R_{ee}^2 = l_B^2 N \ . \tag{5}$$

When $r_s \gg l_B$, the chain persistence length is dominated by the Coulomb contribution $l_p \simeq l_e$. If N is very large such that the chain contour length Nl_B is much larger than l_e then the chain behaves as a linear chain with Nl_B/l_e segments of length l_e each and thickness r_s. The excluded volume between segments is $v \simeq l_e^2 r_s$, and the end-to-end distance[4]:

$$R_{ee}^2 = l_e^2 \left(\frac{v}{l_e^3}\right)^{2/5} \left(\frac{Nl_B}{l_e}\right)^{6/5} \propto \begin{cases} r_s^{4/5} & \text{if } l_e \propto r_s \\ r_s^{6/5} & \text{if } l_e \propto r_s^2 \end{cases} \ . \tag{6}$$

At larger r_s where l_e becomes comparable to the PE contour length, the excluded volume effect is not important. In this case, the chain statistics is again Gaussian and

$$R_{ee}^2 \simeq l_e^2 \frac{Nl_B}{l_e} \propto \begin{cases} r_s & \text{if } l_e \propto r_s \\ r_s^2 & \text{if } l_e \propto r_s^2 \end{cases} \ . \tag{7}$$

Finally, at even larger r_s when l_p is greater than Nl_B, the chain becomes a straight rod with length independent on r_s:

$$R_{ee}^2 \simeq l_B^2 N^2 \ . \tag{8}$$

If $l_e \propto r_s^2$, the transition from the scaling range of Eq. (6) to Eq. (7) happens at $r_s \simeq l_B N^{1/4}$, while the transition from the scaling range of Eq. (7) to Eq. (8) happens at $r_s \simeq l_B N^{1/2}$. On the other hand, if $l_e \propto r_s$, both transitions from the scaling range of Eq. (6) to Eq. (7) and from the scaling range of Eq. (7) to Eq. (8) happen at $r_s \simeq l_B N$. This means, there is no scaling range of Eq. (7) in this theory.

Thus, one can distinguish between the OSF result, $l_p \propto r_s^2$, and the variational result, $l_p \propto r_s$ by plotting the exponent $\alpha = \partial \ln[R_{ee}^2]/\partial \ln r_s$ as a function of $\ln r_s$. The schematic figure of this plot is shown in Fig. 2. OSF theory gives plateaus at $\alpha = 6/5$ and 2, and when $r_s > l_B N^{1/2}$, α drops back to 0. Variational theories, on the other hand, would suggest one large plateau at $\alpha = 4/5$ up to $r_s \simeq l_B N$.

The simulation results for α are shown in Fig. 3 for different N. One can see that as N increases, the agreement with OSF theory becomes more visible. Note that the plateaus in Fig. 2 are scaling ranges, and relatively sharp

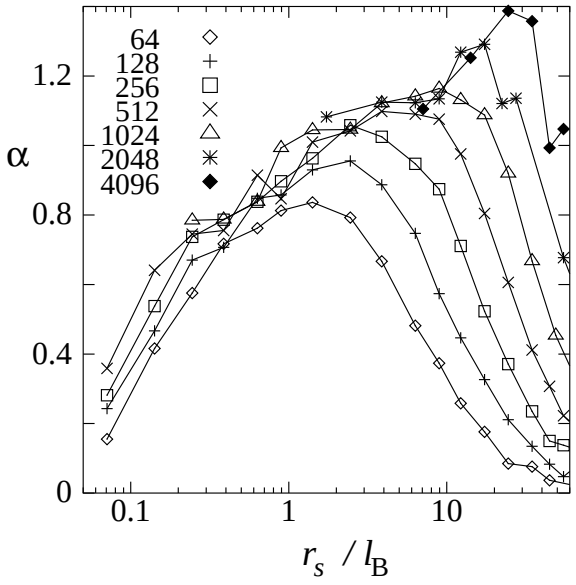

FIG. 3: Simulation result for α as a function of r_s for different N: 64($\diamond$), 128(+), 256 ($\Box$), 512 ($\times$), 1024 ($\triangle$), 2048($*$), and 4096 ($\blacklozenge$). They agree reasonably well with the solid curve of Fig. 2, suggesting that OSF theory is correct.

transitions between plateaus are valid only for $N \to \infty$. For a finite N, the plateaus may be too narrow to be observed and can be masked in the transition regions. This explains why one cannot see the plateau at $\alpha = 2$ in our results. Nevertheless, the tendencies of α to develop a plateau at $\alpha = 6/5$, then to grow higher toward $\alpha = 2$ at larger r_s and finally to collapse to zero when approaching relatively small $r_s = l_B\sqrt{N}$ are clearly seen for large N. Thus, generally speaking, the curves agree with OSF theory much better than with variational theories (where α is supposed to be about 4/5 and to decrease to zero only when $r_s \to l_B N$, i.e. at much larger r_s than what observed).

Fig. 3 also shows one reason why similar simulations done by other groups do not support OSF theory. All of these simulations are limited to 512 charges. As one can see from Fig. 3, the curves for $N \leq 512$ do not permit to discriminate between the two theories as clearly as the case $N = 2048$ or 4096. Only when N becomes very large can scaling ranges with $\alpha > 1$ show up and one observes better agreement with OSF result.

IV. LARGE r_s LIMIT

In this section, we attempt to extract directly from the simulation data the persistence length in order to compare with OSF theory. To do this, one notices that even a chain with excluded volume interaction behaves as a Gaussian chain when its contour length is very short such that it contains only a few Kuhn segments. In this case, one can use the Bresler-Frenkel formula[20] to describe the relationship between the end-to-end distance R_{ee} and the chain persistence length l_p:

$$R_{ee}^2 = 2Ll_p - 2l_p^2[1 - \exp(-L/l_p)] \ , \tag{9}$$

where L is the contour length of the chain.

For our polyelectrolyte, this formula can be used for large r_s when the persistence length is of the order of R_{ee} or larger. However, one cannot use the bare contour length $L_0 = (N-1)l_B$ in the Eq. (9) because the chain where OSF theory is supposed to be applicable is not the bare chain but an effective chain which takes into account local fluctuations. The contour length L of this effective chain is

$$L = Ne/\eta \tag{10}$$

where η is the renormalized linear charge density of the PE.

In KK theory, the effective chain is the chain of electrostatic blobs, and the normalized charge density is $\eta = \eta_0 g l_0/\xi$. However, the standard blob picture can only be used to describe flexible weakly charged chains where the fraction of charged monomers is small so that the number of monomers, g, within one blob is large and Gaussian statistics can be used to relate its size and molecular weight. Because, for a given number of charged monomers, Monte-Carlo simulation for weakly charged polyelectrolyte is extremely time consuming, all monomers of our simulated polyelectrolyte are charged. In this case, the neighbor-neighbor monomers interaction equals k_BT. This makes $g \simeq 1$ and the standard picture of Gaussian blobs does not apply. Thus, in order to treat our data, we assume that both l_p and η are unknown quantities.

To proceed further, one needs an equation relating η and l_p, and in order to verify OSF theory, we could use their formula

$$l_p = \eta^2 r_s^2/4Dk_BT \ , \tag{11}$$

for this purpose. Thus, we could substitute Eq. (10) and (11) into Eq. (9), and solve for η using R_{ee}^2 obtained from simulation. If OSF theory is valid, the obtained values of η should be a very slow changing function of r_s. In addition, in the limit $N \to \infty$, they should also be independent on N.

The OSF equation (3), however, was derived for the case $r_s \ll L$ while in our simulation, the ratio r_s/L is not always small. Therefore, instead of Eq. (11), we use the more general Odijk's finite size formula[1]

$$l_p = \frac{\eta^2 r_s^2}{12Dk_BT}\left[3 - \frac{8r_s}{L} + \left(5 + \frac{L}{r_s} + \frac{8r_s}{L}\right)e^{-L/r_s}\right] . \tag{12}$$

for the persistence length l_p. When $L \gg r_s$, the term in the square brackets is equal to 3 and the standard OSF result is recovered. On the other hand, when $r_s \gg L$, the persistence length l_p saturates at $\eta^2 L^2/72Dk_BT$.

Below, we treat our Monte-Carlo simulation data with the help of Eq. (9) using Eq. (10) and (12) for L and

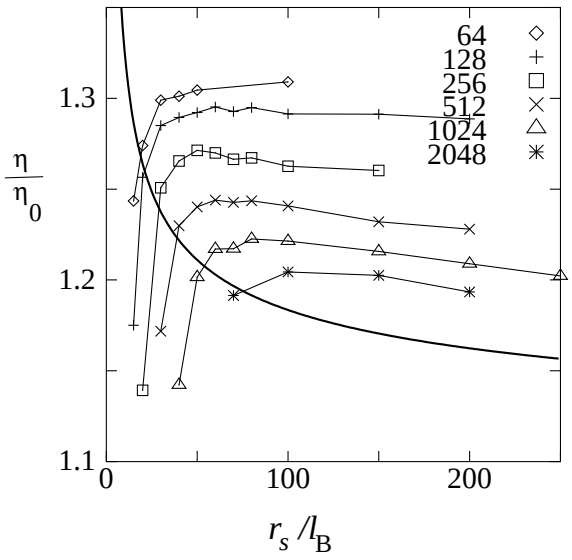

FIG. 4: The linear charge density η as a function of the screening length for different N: 64($\diamond$), 128(+), 256 ($\Box$), 512 ($\times$), 1024 ($\triangle$) and 2048($*$). The thick solid line is the theoretical estimate which is the numerical solution to Eq. (13), (14) and (15).

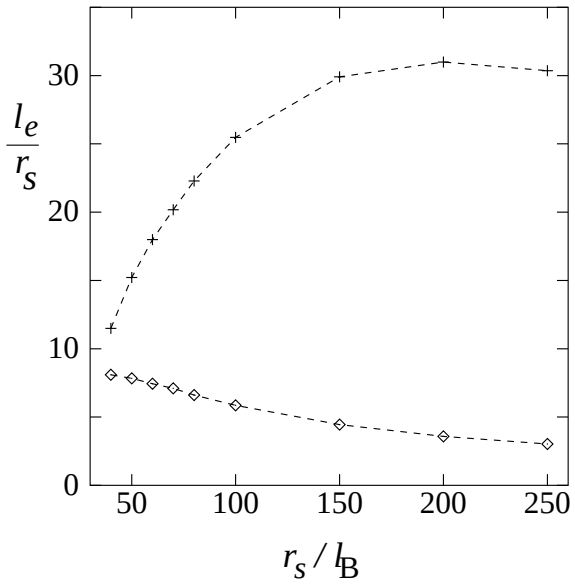

FIG. 5: Plots of l_e/r_s as a function of r_s calculated with the help of Eq. (9), (10) and (12) using our data for R_{ee}^2 (+) and using unperturbed $\eta = \eta_0$ as in Ref. 15 ($\diamond$). The chain with $N = 1024$ is used.

l_p. The results for η are plotted in Fig. 4 for different PE sizes N. As one can see, at large r_s, η changes very slowly with r_s, and as N increases, tends to saturate at an N independent value.

It should be noted that the lines $\eta(r_s)$ in Fig. 4 unphysically start to drop below certain values of r_s. This is because at smaller r_s, the electrostatics-induced excluded volume interactions between monomers become so strong that the right hand side of Eq. (9) (which is derived for a Gaussian worm like chain) strongly underestimates R_{ee}.

Even though the picture of Gaussian blobs does not work for our chain, η can still be calculated analytically in the limit $L \gg r_s$ ($N \to \infty$). Indeed, let us assume that the effective chain is straight at length scale smaller than r_s (which is a reasonable assumption because all the analytical theories so far suggested that the PE persistence length scales as r_s or r_s^2). Thus, the self energy of the chain can be written as $E = L\eta^2 \ln(r_s/l_B)/D$. At length scale smaller than r_s, the polyelectrolyte behaves as a neutral chain under an uniform tension

$$F = \partial E/\partial L = \eta^2 \ln(r_s/l_B)/D \ . \tag{13}$$

The average angle a bond vector makes with respect to the axis of the chain, therefore, is:

$$\begin{aligned} \langle \cos\theta \rangle &= \frac{\int_0^\pi \exp(Fl_B \cos\theta/k_BT) \cos\theta \sin\theta d\theta}{\int_0^\pi \exp(Fl_B \cos\theta/k_BT) \sin\theta d\theta} \\ &= \coth \frac{Fl_B}{k_BT} - \frac{k_BT}{Fl_B} \ . \end{aligned} \tag{14}$$

The charge density η can be calculated as

$$\eta = \eta_0 / \langle \cos\theta \rangle \ . \tag{15}$$

At weak screening $r_s \gg l_B$, it can be estimated analytically:

$$\eta \simeq \eta_0 \left[1 + \frac{1}{\ln(r_s/l_B)} + ... \right] \ , \tag{16}$$

where the expansion terms of the order of $1/\ln^2(r_s/l_B)$ and higher were neglected.

The more accurate numerical solution of Eq. (13), (14) and (15) for η is plotted in Fig. 4 by the thick solid line. One can see that the values $\eta(r_s)$ calculated experimentally using OSF theory with growing N converge well to the theoretical curve for $N = \infty$. Remarkably, the theoretical estimate for η does not use any fitting parameters. This, once again, strongly suggests the OSF theory is valid for flexible PE as well.

The Bresler-Frenkel formula, Eq. (9), is also used to extract the persistence length in Ref. 15 where the authors concluded that the dependence of l_e on r_s is sublinear. The authors, however, used in Eq. (9) the bare contour length L, or in other words $\eta = \eta_0$, for the calculation of l_e. As one can see from Fig. 4, this leads to 20-30% overestimation of the contour length of the effective chain where OSF theory is supposed to apply. To show that this overestimation is crucial, let us treat our data similarly to Ref. 15 using $\eta = \eta_0$. We plot the resulting dependence of l_e/r_s on r_s (similarly to Fig. 4 of Ref. 15) and compare it with our own results using corrected η. The case $N = 1024$ is shown in Fig. 5. Obviously, the two results are different qualitatively. While the upper curve follows Eq. (12) with slightly decreasing η, the lower curve shows sublinear growth of l_e with r_s (l_e/r_s is a decreasing function of r_s). This sublinear dependence observed in Ref. 15 is clearly a manifestation

of their overestimation of the PE length L which should be used in Eq. (9).

Note that the true l_e/r_s curve should also eventually decrease to zero because l_e saturates to the constant value $\eta^2 L^2/72Dk_BT$ when $r_s \gg L$ [See Eq. (12)]. But, according to Eq. (12), this decay starts only at very large r_s where $r_s/L \simeq 0.25$. The deviation from $l_e \propto r_s^2$ at large r_s seen in Fig. 5 is due to both the violation of the inequality $r_s \ll L$ and to the slight decrease of η with r_s.

V. BOND ANGLE CORRELATION FUNCTION

Another standard procedure used in literature is to calculate the persistence length of a polyelectrolyte as the typical decay length of the bond angle correlation function (BACF) along the contour of the chain, assuming the later is exponential.

$$f(|s'-s|) = \langle \cos[\angle(\mathbf{b}_s, \mathbf{b}_{s'})] \rangle \propto \exp\left(-\frac{|s'-s|}{l_p}\right) \ . \quad (17)$$

Here $\mathbf{b}_s$ and $\mathbf{b}_{s'}$ are the bond numbered s and s' respectively and $\angle(\mathbf{b}_s, \mathbf{b}_{s'})$ is the angle between them. The symbol $\langle ... \rangle$ denotes the averaging over different chain conformations. To improve averaging, the pair s and s' are also allowed to move along the chain keeping $|s'-s|$ constant.

We argue in this section that this method of determining persistence length actually has a very limited range of applicability. At either small or large r_s, the results of persistence length obtained from BACF are not reliable. In the range where this method is supposed to be applicable, we show that the obtained l_p are close to those obtained in Sec. IV above.

For small r_s, excluded volume plays important role and, strictly speaking, it is not clear whether BACF is exponential, and if yes, how one should eliminate excluded volume effect and extract l_p from the decay length. According to Ref. 14, the decay is not exponential in this regime.

The procedure of determining the persistence length using BACF becomes unreliable at large r_s as well. To elaborate this point, in Fig. 6a, we plot the logarithm of the bond angle correlation function $f(x)$ along the PE contour length for a $N = 512$ and $r_s = 50l_B$, typical values of N and r_s where the excluded volume due to Coulomb interactions is small. There are three regions in this plot. In region A at very small distance along the PE contour length, monomers are within one electrostatic blobs from each other and the effects of Coulomb interaction are small. The bond angle correlation in this region decays over one bond length l_B. At larger distance along the PE contour length, the region B, the decay is exponential and a constant decay length seems well-defined. Finally, at distance comparable to the chain's contour length, one again observes a fast drop of the BACF (region C). This end effect is due to the fact that the stress at the end of the chain goes to zero and the end bonds become uncorrelated. The persistence length of interest can be defined as the decay length in region B.

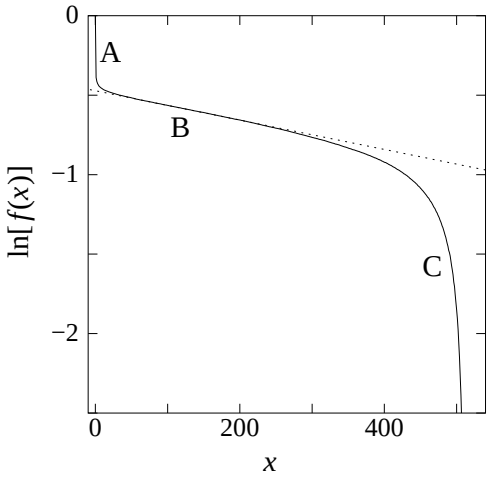

FIG. 6: The logarithm of the bond correlation function $f(x)$ as a function of the distance x (in units of l_B) along the chain for the case $N = 512$, $r_s = 50l_B$. There are three regions A, B and C. The dotted line, $-0.47 - x/1083$, is a linear fit of region B suggesting that the persistence length for this case is $l_p = 1083l_B$.

TABLE I: Comparison between l_{BACF} calculated using BACF method and $\eta l_e/\eta_0$ calculated in Sec. IV. All lengths are measured in units of l_B.

N	r_s	l_{BACF}	$\eta l_e/\eta_0$
2048	100	4590	3682
	150	9000	7484
1024	80	2535	2180
	100	3733	3111
512	50	1083	809

Problem arises, however, at large enough r_s when the region C (the end effect) becomes so large that region B is not well defined. In this case the obtained decay length underestimates the correct persistence length. As one can see from Fig. 6, region C can be quite large. It occupies 40% of the available range of x, even though the screening length is only 10% of the contour length in this case.

There is an even more strict condition on how large r_s is when the method of BACF loses its reliability. If l_e is larger than L, the decrease of $\ln f(x)$ in region B is less than unity. When this happens, an exponential decay is ambiguous.

Because of all these limitations, in this section we use BACF to calculate l_e only in the very limited range of r_s where excluded volume is not important and l_e is not much larger than L (the decrease in region B is greater than 0.1). The obtained l_{BACF}, which is measured along the chain contour, is compared to $\eta l_e/\eta_0$ obtained using

the Bresler-Frankel formula in the previous subsection. (The factor η/η_0 is needed because l_{BACF} is measured along the real PE contour while l_e is measured along the renormalized PE contour.) The results are shown in the Table I. The two persistence lengths are within 20-25% of each other. This reasonably good agreement between two different methods shows that our calculations are consistent. It further strengthens the conclusion of two previous sections that OSF theory is correct in describing flexible polyelectrolytes.

VI. CONCLUSION

In this paper, we use extensive Monte Carlo simulation to study the dependence of the electrostatic persistence length of a polyelectrolyte on the screening radius of the solution. Not only did we simulate a much longer polyelectrolyte than those studied in previous simulations in order to show the scaling ranges, we also used a refined analyses which take into account local fluctuations to calculate the persistence length. These improvements result in a good support for OSF theory. They also help to explain why previous simulations failed to support OSF theory.

In order to describe our numerical data we used a modified OSF theory in the framework of ideas of KK. Linear charge density η was corrected to allow for short range fluctuations. In our case this is a relatively small correction to η_0 because we deal with a strongly charged PE. When one crosses over to sufficiently weakly charged PE linear charge density becomes strongly renormalized and matches KK expressions. We confirmed that corrections of η do not affect r_s^2 dependence of persistence length which was predicted by OSF for $l_0 \ll r_s \ll L$. In other words, we confirm KK idea that at large r_s all effects of flexibility of PE are limited to a renormalization of η. At r_s comparable to contour length L we found a good agreement of the numerical data with OSF formula modified for this case [Eq. (12)], which is derived in Ref. 1. Again all effects of local flexibility are isolated in the small correction to the linear charge density η.

Acknowledgments

The authors are grateful to A. Yu. Grosberg M. Rubinstein, M. Ullner and R. Netz for useful discussions and comments. This work is supported by NSF No. DMR-9985785. T.T.N. is also supported by the Doctoral Dissertation Fellowship of the University of Minnesota.

[1] T. Odijk, J. Polym. Sci., Polym. Phys. Ed. **15** (1977) 477.
[2] J. Skolnick, and M. Fixman, Macromolecules **10** (1977) 944.
[3] J.-L. Barrat, and J.-F. Joanny, Europhys. Lett. **24** (1993) 333; J.-L. Barrat, and J.-F. Joanny, Adv. Chem. Phys., **94** (1996) 1.
[4] A. R. Khokhlov, and K. A. Khachaturian, Polymer **23** (1982) 1793.
[5] Hao Li, and T. A. Witten, Macromolecules **28** (1995) 5921.
[6] R. R. Netz, and H. Orland, Eur. Phys. J. B **8**, 81 (1999).
[7] B. -Y. Ha, and D. Thirumalai, J. Chem. Phys. **110**, 7533 (1999).
[8] D. Bratko, and K. A. Dawson, J. Chem. Phys. **24** (1993) 5352.
[9] B. -Y. Ha, and D. Thirumalai, Macromolecules **28** (1995) 577.
[10] J. L. Barrat, and D. Boyer, J. Phys. II France **3** (1993) 343.
[11] C. E. Reed, and W. F. Reed, J. Chem. Phys. **94**, 8479 (1991).
[12] C. Seidel, Ber. Bunsen-Ges. Phys. Chem. **100**, 757 (1996).
[13] M. Ullner, B. Jönsson, C. Peterson, O. Sommelius, and B. Söderberg, J. Chem. Phys. **107**, 1279 (1997);
[14] M. Ullner, and C. E. Woodward, Macromolecules **35**, 1437 (2002).
[15] U. Micka, and K. Kremer, Phys. Rev. E **54** (1996) 2653.
[16] M. Ullner, in "Handbook of Polyelectrolytes and Their Applications", J. Kumar S. Tripathy and H. S. Nalwa, eds, American Scientific Publishers, Los Angeles (2002).
[17] T. T. Nguyen, and B. I. Shklovskii, cond-mat/0202168.
[18] R. Everaers, A. Milchev, and V. Yamakov, cond-mat/0202199.
[19] M. Lal, Mol. Phys. **17**, 57 (1969); N. Madras and A. D. Sokal, J. Stat. Phys. **50**, 109 (1988); B. Jönsson, C. Peterson, and B. Söderberg, J. Phys. Chem. **99**, 1251 (1995); M. Ullner, B. Jönsson, B. Söderberg, and C. Peterson, J. Chem. Phys. **104**, 3048 (1996).
[20] L. D. Landau, and E. M. Lifshitz, *Statistical Physics*, Butterworth and Heinemann, Oxford, 1996.